Reanalysis of the ionospheric total electron content anomalies around the 2011 Tohoku-Oki and 2016 Kumamoto earthquakes: Lack of a clear precursor of large earthquakes

Ryoya Ikuta, Ryoto Oba, Daiki Kiguchi and Tomoya Hisada

Abstract:

We investigate the veracity of the reports by Iwata & Umeno (2016, https://doi.org/10.1002/2016JA023036) and Iwata & Umeno (2017, https://doi.org/10.1002/2017JA023921), both of which claimed that the observed perturbations in GNSS-based ionospheric total electron content (TEC) could serve as a "precursor" of large earthquakes based on correlation analysis. Iwata&Umeno (2016) defined the spatial correlation of the residuals between the observed and predicted TEC time series and reported that the values are significantly larger before large earthquakes than those observed during non-earthquake periods. Iwata&Umeno (2017) claimed that the preseismic ionospheric disturbances can be distinguished from other non-earthquake phenomena based on the small percentage of area where the correlation value exceeds the criterion. They also claimed that the low propagation velocity of the correlation peaks is also a pre-seismic characteristic. Here we test their claims using a larger dataset. As a result, these three characteristics they claimed to have captured as evidence of earthquake precursors are not significant being frequently observed during

normal (non-earthquake) days, and therefore we can find no basis for claiming that they are precursors to the earthquakes.

Introduction

Numerous studies have reported on the existence of the precursory enhancement of total electron content (TEC) as a precursor of large earthquakes (e.g., Heki, 2011; Heki and Enomoto, 2015; He and Heki, 2017), whereas other studies have doubted its existence (e.g., Kakinami et al., 2012; Kamogawa and Kakinami, 2013; Utada and Shimizu, 2014; Ikuta et al., 2020). However, the proponents cannot prove that TEC enhancement is a true precursor, and the opponents cannot prove that this is not a precursor. This is because of the general noisiness of the ionosphere, which causes the TEC fluctuation that is labeled a precursor to be indistinguishable from usual disturbances of space weather origin. We can only discuss how the observed anomalies are different from those observed on non-earthquake days, or whether there is a very low probability that the anomalies were observed during the earthquake by chance based on the frequency of the observations on non-earthquake days.

Iwata & Umeno (2016; hereafter I&U16) and Iwata & Umeno (2017; hereafter I&U17) have recently proposed a correlation analysis of TEC time series between Global Navigation Satellite System (GNSS) stations, and claimed to have successfully

identified the emergence of precursory TEC anomalies approximately 1 hour before both the 11 March 2011 Mw 9.0 Tohoku-Oki earthquake (I&U16) and 15 April 2016 Mw 7.3 Kumamoto earthquake (I&U17). I&U16 have claimed that they were able to detect precursory TEC changes with high correlation values (up to C(T)=25), which are much larger than the usual upper limit (C(T)=5), such that these precursory earthquake signals can be distinguished from other signals. In addition to the 2011 Tohoku-Oki earthquake, they detected an anomalous area prior to three of the four studied M7-class earthquakes based on slightly lower correlation values than those determined for the Tohoku-Oki earthquake case. I&U17 applied the same procedure to the TEC time series before the 2016 Kumamoto earthquake, and claimed to have detected a precursory TEC correlation change. They also provided two new indicators for distinguishing precursory TEC anomalies from those of space weather origin: those are “anomalous area rates” and those that are “C(T) propagation velocities”.

We highlight three problems that arise in the two papers. The first is the degree of inconsistency between the two papers. The characteristics of the earthquake precursor reported in I&U16, which is a remarkably large C(T) that is five times larger than the maximum correlation values for several non-earthquake days was treated as an unremarkable observation in I&U17 since these values were observed during most of

57 the eight non-earthquake days. I&U17 adopted a completely different set of criteria
58 from I&U16 and did not check whether or not the TEC anomaly prior to the Tohoku-
59 Oki earthquake in I&U16 met the new criteria or not. The second problem is the lack of
60 data during the non-earthquake days. I&U16 only showed the C(T) values for one
61 satellite during four non-earthquake days to highlight their low values. However,
62 I&U17 found many days with high C(T) values, including some that were even higher
63 than that before the Tohoku-Oki earthquake. The claim of significant, large C(T) values
64 in I&U16 would not have been possible if a comprehensive analysis of the data,
65 including more satellite-station pair and days, was undertaken. I&U17 also lacked data
66 analysis of non-earthquake-day C(T) values to fully validate their new criteria.
67 Although I&U17 analyzed the TEC data for one earthquake day and 12 non-earthquake
68 days, the presented results were deduced using only two satellites during seven days to
69 evaluate the first “anomalous area rate” criterion and only one satellite during four days
70 to evaluate the second “propagation velocities” criterion; these are too few data to be
71 treated statistically. The third problem is the loose criteria and/or lack of quantification
72 in I&U17. They introduced the anomalous area rate criterion based on an idea that the
73 anomalous area is smaller in the case of an earthquake precursor than in the case of a
74 signal of space weather origin. However, their own diagrams (Figure 9 and Figure 10 in

I&U17) illustrated that the non-earthquake days possessed comparable anomalous area rates to that on the earthquake day. I&U17 also showed that the C(T) peak around the focal area of the Kumamoto earthquake propagated more slowly than seasonal medium-scale traveling ionospheric disturbances (MSTIDs), and defined this as the propagation velocity criterion. However, the velocities they provided as an indicator to distinguish an earthquake precursor form MSTIDs were 65–168 m/s, which is within the MSTID propagation velocity range.

Here we examine the correlation method developed by I&U16 and I&U17 by applying it to the days without a large earthquake to evaluate the significance of the reported correlation values, anomalous area rates, and propagation velocities before the Tohoku and the Kumamoto earthquakes.

Data Processing

We first calculated the vertical TEC (VTEC) from the Global Navigation Satellite System (GNSS) phase data provided by the geospatial information authority of Japan. We then applied the method proposed by I&U16 to the same dataset they analyzed to ensure that we reproduced their method correctly. Here we provide a brief explanation of the procedure; see I&U16 for full details. A portion of the VTEC time series is first

93 fitted with a regression curve, which is designed to predict VTEC at a future time. The
94 difference between the observed and predicted VTEC values in the future time is
95 recognized as an anomaly $x(t)$. The correlation between $x(t)$ at a central GNSS station
96 and its surrounding 30 stations are then calculated. The average of the correlations for
97 the 30 pairs is regarded as C(T). We fit the training data in the 120-min-long time
98 window (240 samples) with a septic function to predict the data in the future 15 min (30
99 samples) during the $x(t)$ calculation. These functions and parameter sets are the same as
100 those in I&U16. Although I&U16 suggested that they can choose a range of functions
101 and parameters, and presented differences in the resulting C(T) values between various
102 functions and parameters, they only quantitatively evaluated the significance of their
103 result for this parameter sets.
104

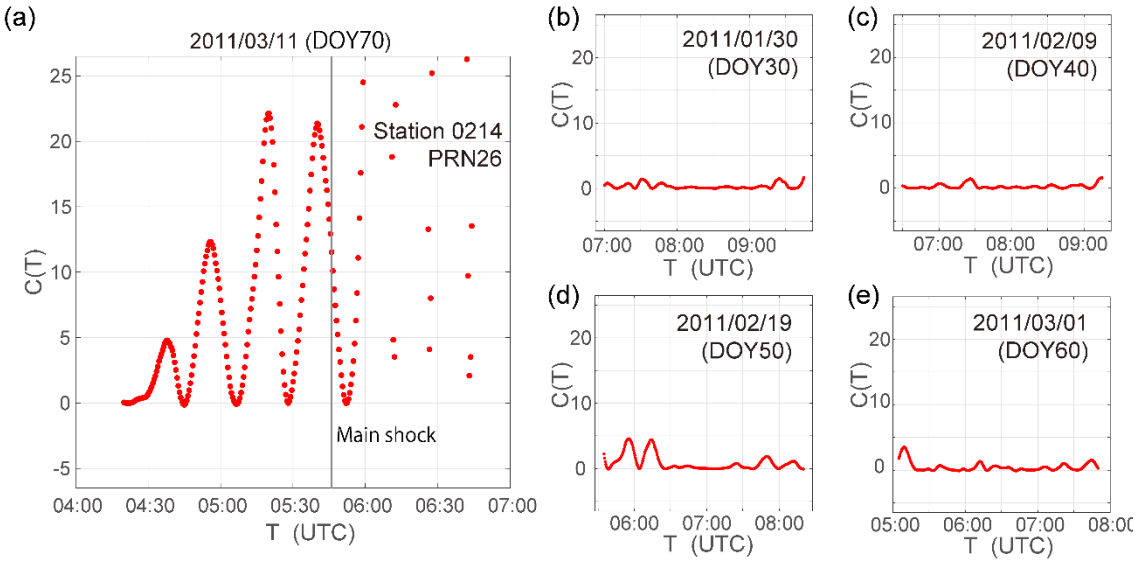

Figure 1. Reproduction test of Figure 1 and Figure 3 in I&U16 using the same satellite-central station pair as theirs. The central station is Kitaibaraki (0214), the satellite is PRN26. The regression curves are septic functions. (a) The day of Tohoku-Oki earthquake. The time of the mainshock is indicated by the vertical line. (b) Forty days (DOY30), (c) 30 days (DOY40), (d) 20 days (DOY50), and (e) 10 days (DOY60) before the earthquake. They are good reproductions of I&U16.

Results

C(T)s in non-earthquake days focused by Iwata & Umeno (2016)

Figure 1 shows calculated C(T) time series for satellite PRN26, and Kitaibaraki (0214) GNSS station (central station) and its 30 surrounding stations on the day of the 2011 Tohoku-Oki earthquake (day of year (DOY) = DOY70) and four selected non-earthquake days (DOY30, 40, 50, and 60 in 2011). These C(T) variations are similar to those in figures 1 and 3 of I&U16. The C(T) variations on the earthquake day are about five times larger than those on the non-earthquake days, as I&U16 claimed. Even

though the C(T) value before the Tohoku-Oki earthquake (Figure 1a) is smaller in our result (22.5) than theirs (25), the variation patterns are very similar. This discrepancy may be due to small differences in the data analysis, such as the number of samples in the 15-min time series (30 or 31), the number of available GNSS stations (out of 30), the inter-frequency bias (IFB) station corrections during the VTEC pre-processing, and other items that are not outlined in I&U16. We also apply this C(T) calculation to additional data to test their claims.

We examine C(T) time series during these days at the stations not shown in I&U16 to determine if C(T) is really as small as they reported. We adopt an elevation mask angle of 20 degrees for our C(T) calculation to suppress any unrealistic C(T) increases due to large VTEC variation near the horizon. This means that we do not calculate C(T) if the elevation angle is less than 20 degrees for any part of the 135-min time series of the data. Furthermore, a station is not used as the central station if the 30 surrounding stations do not fall within a 100-km radius of that station.

Figure 2 shows the time series of the maximum C(T) over Japan. The maximum C(T) values during these non-earthquake days often exceeds five and sometimes reaches 100. However, I&U16 appeared to ignore these large C(T) values. The maximum C(T) was especially large on the day of the earthquake (DOY70: Figure 2a) compared with the

other days, but the value on the 04:45–05:45 (UTC) interval, which was focused on in I&U16 to infer the earthquake precursor (Figure 1a), is relatively small whereas the 02:00-4:00 (UTC) interval possessed significantly larger maximum C(T) values. The large C(T) during the day of the earthquake (DOY70) might have been due to the relatively high geomagnetic activity, as suggested by the Kp index provided by the German Research Centre for Geosciences. The average geomagnetic activity indices Kp for the 00:00 to 09:00 (UTC) interval on DOY30, DOY40, DOY50, DOY60 and DOY70 were 0+, 0, 2, 3− and 5, respectively, with DOY70 possessing a significantly larger Kp value than the other days. A frequency histogram of the maximum C(T) for the 02:00−10:00 (UTC) interval during nine non-earthquake days in 2011 (DOY30, DOY31, DOY40, DOY49, DOY50, DOY60, DOY63, DOY72, and DOY73) is shown in Figure 3a. The C(T) values for the non-earthquake days are not necessarily small, as I&U16 claimed. Therefore, our more comprehensive analysis indicates that the precursory C(T) increase reported by I&U16 with satellite PRN26 at GNSS station 0214 before the 2011 Tohoku-Oki earthquake is not significantly large compared with the C(T) increases during other periods.

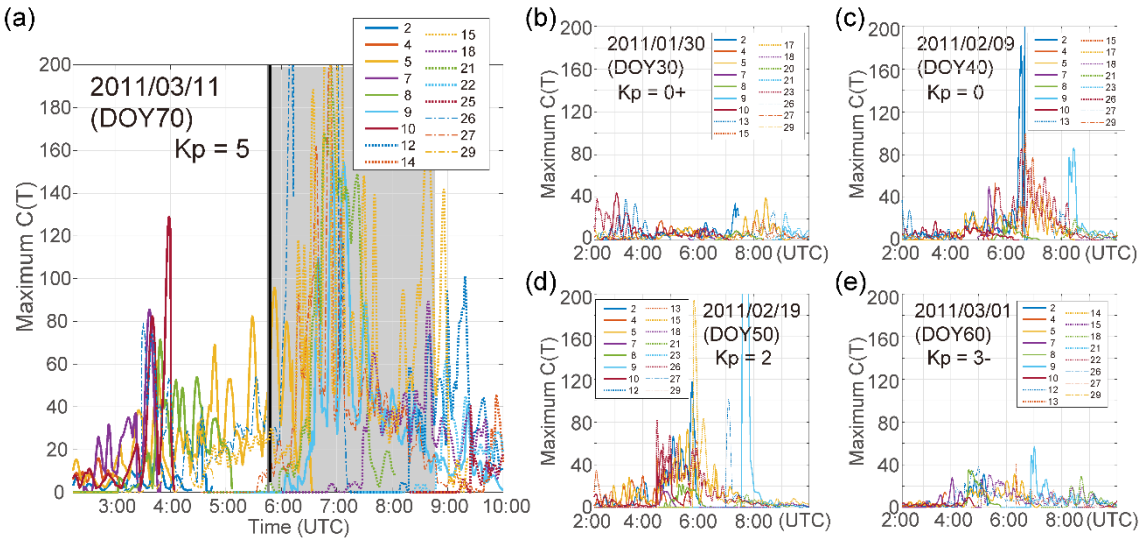

Figure 2. Time series of the maximum C(T) values for each of the satellites and all of the GNSS stations in Japan. (a) The day of the 2011 Tohoku-Oki earthquake (DOY70). The time of the main shock is indicated by the vertical line. The C(T) values in the shaded period (05:46–08:46 UTC) are not counted in Figure 3a to avoid the post-seismic ionospheric disturbances. (b) Forty days (DOY30), (c) 30 days (DOY40), (d) 20 days (DOY50), and (e) 10 days (DOY60) before the earthquake.

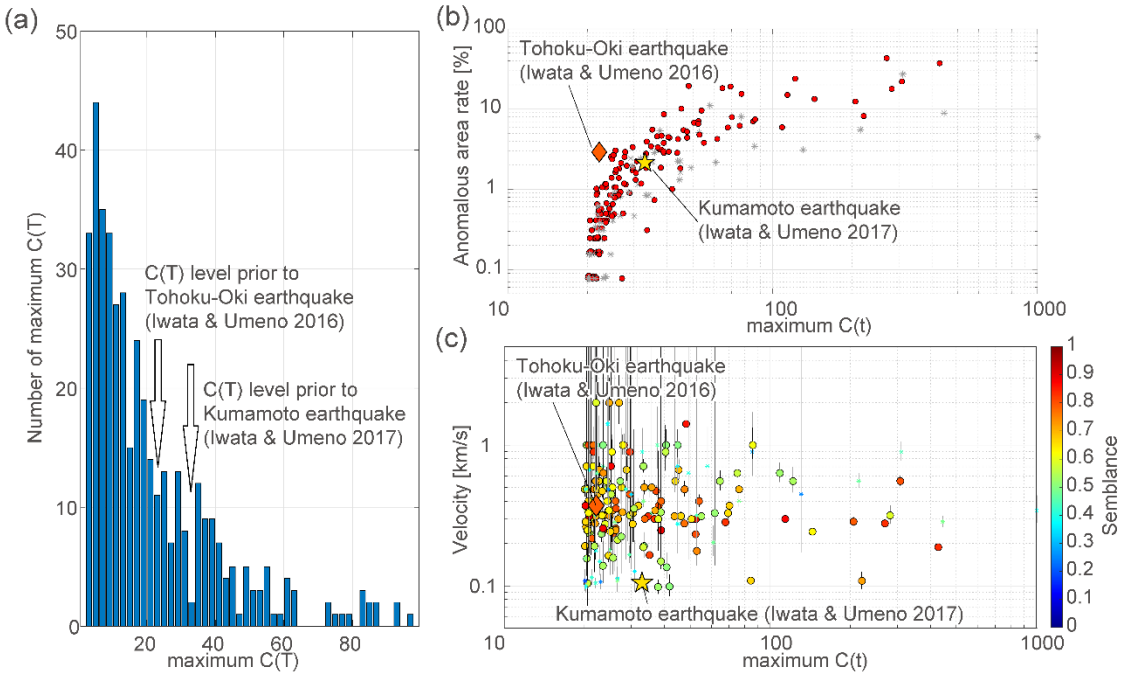

Figure 3. (a) Histograms of hourly maximum C(T) during the 02:00–10:00 (UTC) interval of nine non-earthquake days (DOY30, DOY31, DOY40, DOY49, DOY50, DOY60, DOY63, DOY72, and DOY73 in 2011). The C(T) frequency is in the 2–100 range (interval = 2). The large pre-seismic C(T) values reported by I&U16 and I&U17 which are shown by the arrows, are not significant signal due to the number of similar and larger C(T) values. Note that there are 24 maximum C(T) values larger than 100 that are not shown in the figure. (b) Anomalous area rate against the C(T) peak value. Red circles show the daytime values for 12 non-earthquake days (11:15-19:00 local time (LT) for DOY30, DOY31, DOY40, DOY49, DOY50, DOY60, DOY63, DOY72, and DOY73 in 2011, and DOY96, DOY106, and DOY116 in 2016) and the nighttime values for two non-earthquake days (19:15–05:00 LT of DOY96

and DOY116 in 2016) against C(T) peak values. Red circles and asterisks indicate the C(T) peaks in the non-earthquake days with semblance values of >0.5 and <0.5, respectively. The low semblance values suggest that the variation in C(T) does not follow the assumed plane-wave propagation. The diamond marks the value that was calculated at 05:20 UTC using satellite PRN26 and central station 0214 before the 2011 Tohoku-Oki Earthquake (05:46 UTC), which was reported by I&U16. The star marks the value that was calculated at 16:09 UTC using satellite PRN17 and central station 0087 before the 2016 Kumamoto Earthquake (16:25 UTC), which was reported by I&U17. (c) C(T) peak propagation velocities for the peak values. Circles show the values during the same 11 non-earthquake days shown in Figure 3b. The circles are color-coded to show semblance values that were calculated using stations within 200 km of the central station with the maximum C(T) value. The diamond shows the value calculated using satellite PRN26 and central station 0214 before the Tohoku-Oki earthquake (04:45–05:45 UTC). The star shows the value that was calculated using satellite PRN17 and central station 0087 before the 2016 Kumamoto Earthquake (15:25–16:25 UTC).

156

157 **Anomalous area rate and propagation velocities focused by Iwata & Umeno (2017)**

158 We next test the significance of the anomalous area rate criterion proposed by I&U17.
159 They claimed that the anomalous area rate, which is the percentage of stations with
160 C(T) above a threshold (20) among all of the GNSS stations, clearly proves that
161 earthquake days and non-earthquake days possess significantly different C(T) values
162 based on the data for nine days: the earthquake day (15 April 2016) and eight non-
163 earthquake days (1–5 January and 12–14 April 2016). They showed that large C(T)
164 values occurred within a relatively limited number of stations (~10 %) during the
165 earthquake day, and interpreted that these observations were due to the fact that these
166 precursory earthquake anomalies occur within a narrower range than those caused by
167 MSTIDs. They claimed that large anomalous area rates were seen on days when
168 MSTIDs were observed. However, small anomalous area rates were not only seen on
169 the earthquake day. For example, small anomalous area rates (<10%) were observed on
170 12 April, 14 April, and 3 January in figure 9 of I&U17 that were comparable with that
171 for the earthquake day. We test their claim based on the C(T) values that were
172 calculated during the daytime for 12 non-earthquake (11:15–19:00 LT for DOY30,
173 DOY31, DOY40, DOY49, DOY50, DOY60, DOY63, DOY72, and DOY73 in 2011,
174 and DOY96, DOY106, and DOY116 in 2016) and during the nighttime for two non-
175 earthquake days (19:15–05:00 LT for DOY96 and DOY116 in 2016) against the C(T)

peak values. Figure 3b shows the anomalous area rates when the maximum C(T) value exceeded 20. The anomalous area rates are generally proportional to the maximum C(T). We can see that there are many cases where the maximum C(T) exceeded 30 whereas the anomaly rate was <5% for these 14 non-earthquake periods. The pre-seismic values for the Tohoku-Oki and Kumamoto earthquakes do not appear to be either significant or unique, as they are buried among other values that are observed during non-earthquake periods.

We finally test their claim of the low propagation velocity of the C(T) peak. The propagation velocities of the C(T) peaks discussed above are estimated via semblance analysis. Semblance analysis is a method of determining the velocity of a propagating wave using an array of observation stations. We assume that the target wave propagates at a constant velocity, such that the time of the waveform at each station is shifted by the time difference based on the assumed velocity vector, with the shifted waveforms for each station then summed according to the following semblance equation:

$$c(\tau, p, q) = \frac{\sum_{k=-K/2+1}^{K/2} \left\{ \sum_{i=1}^{M} C_i(\tau + k\Delta\tau - px_i - qy_i) \right\}^2}{M \sum_{k=-K/2+1}^{K/2} \sum_{i=1}^{M} C_i(\tau + k\Delta\tau - px_i - qy_i)^2}, \quad (1)$$

where $\Delta\tau$ is the sampling interval [30 s], x_i and y_i are east–west and north–south

192 coordinates of the *i*-th station in the array with respect to a reference station [m],
193 respectively; p and q are the assumed eastward and northward slowness of the
194 propagating wave [s/m]; K is the number of samples in the time series; and M is the
195 number of stations used to calculate the semblance. Here we define K as 120 (60 min)
196 and M as the number of stations located within 200 km of the reference station. Figure
197 3c shows the estimated propagation velocities of the C(T) peaks. The C(T) propagation
198 velocities observed before the Tohoku-Oki and Kumamoto earthquakes are estimated to
199 be 0.37 ± 0.03 km/s and 0.11 ± 0.01 km/s, respectively. Therefore, the propagation
200 velocity before the 2011 Tohoku-Oki Earthquake is typical of the propagation velocity
201 distribution of the non-earthquake periods shown in Figure 3c, whereas the propagation
202 velocity before the 2016 Kumamoto Earthquake is close to the lower limit of those
203 observed during the non-seismic periods. However, neither of these suggested
204 earthquake precursor signals possess values that are not seen during the non-seismic
205 periods. The claim by I&U17 that C(T) only exhibits a prominent feature in the pre-
206 seismic case is therefore incorrect. Previous studies have indicated that the 65–168 m/s
207 pre-seismic MSTID velocity range reported by I&U17 is not abnormally low (e.g.,
208 Thome, 1964; Hansucker, 1982). For example, Hernández-Pajares et al. (2006)
209 estimated 50–400 m/s MSTID propagation velocities for 400–1200-s period signals

observed using the GNSS network.

We can find no evidence that I&U16 and I&U17 have definitively captured the precursors of the two large earthquakes as they claimed, in terms of either the C(T) magnitude, anomalous area ratio, or C(T) propagation velocity.

References

Heki, K. (2011), Ionospheric electron enhancement preceding the 2011 Tohoku-Oki earthquake, *Geophys. Res. Lett.*, **38**, L17312.

Heki, K. & Enomoto, Y. (2015), Mw dependence of pre-seismic ionospheric electron enhancements, *J. Geophys. Res., Space Physics*, **120**, 7006-7020.

He, L. & Heki, K. (2017), Ionospheric anomalies immediately before Mw 7.0-8.0 earthquakes, *J. Geophys. Res., Space Physics*,**122**, 8659–8678.

Herna´ndez-Pajares, M., J. M. Juan, and J. Sanz (2006), Medium-scale traveling ionospheric disturbances affecting GPS measurements: Spatial and temporal analysis, *J. Geophys. Res., Space Physics*, **111**, A07S11, doi:10.1029/2005JA011474.

Hunscker, R. D. (1982), Atmospheric gravity waves generated in the high-latitude ionosphere: A review, *Review of Geophysics and Space Physics*, **20**, 2, 239-315

Ikuta, R., Hisada, T., Karakama, G., & Kuwano, O. (2020). Stochastic evaluation of pre-earthquake TEC enhancements. *Journal of Geophysical Research: Space Physics*, *125*, e2020JA027899. doi:10.1029/2020JA027899.

232 Iwata, T., and Umeno, K. (2016), Correlation analysis for preseismic total electron
233 content anomalies around the 2011 Tohoku-Oki earthquake, *J. Geophys. Res.,*
234 *Space Physics*, 121, 8969–8984, doi:10.1002/2016JA023036.
235 Iwata T., and Umeno, K. (2017), Preseismic ionospheric anomalies detected before the
236 2016 Kumamoto earthquake, *J. Geophys. Res. Space Physics*, *122*, 3602–3616,
237 doi:10.1002/2017JA023921.
238 Kakinami, Y., Kamogawa, M., Tanioka, Y., Watanabe, S., Gusman, A. R., Liu J-Y.,
239 Watanabe, Y., & Mogi, T. (2012), Tsunamigenic ionospheric hole, *Geophys. Res.*
240 *Lett.*, 39, L00G27, doi:10.1029/2011GL050159.
241 Kamogawa, M. & Kakinami, Y. (2013), Is an ionospheric electron enhancement
242 preceding the 2011 Tohoku-oki earthquake a precursor?, *J. Geophys. Res.*, *Space*
243 *Physics*, 118, 1-4, doi:10.1002/jgra.50118.
244 Thome G. D. (1964), Incoherent scatter observations of traveling ionospheric
245 disturbances, *J. Geophys. Res.*, **69**, 19, 4047-4049
246 Utada, H., and H. Shimizu (2014), Comment on "Preseismic ionospheric electron
247 enhancements revisited" by K. Heki and Y. Enomoto, *J. Geophys. Res.*, *Space*
248 *Physics*, **119**, 6011–6015, doi:10.1002/2014JA020044.
249